Statistics Netherlands

2018 Scientific Paper

Improved time resolution relationship between pressure and earthquake rates in Groningen

Jan. 2018

Frank P. Pijpers

Contents

Nederlands

Deze rapportage is een verslag van onderzoek dat is uitgevoerd in het kader een onderzoeksproject door het CBS in opdracht van Staatstoezicht op de Mijnen (SodM) sinds 2014. Dit onderzoek is ten behoeve van een statistische onderbouwing van het meet- en regelprotocol voor optimale gasexploitatie in de provincie Groningen, met in het bijzonder de aandacht gericht op de relatie tussen de gasdruk in het reservoir, die in de tijd varieert vanwege de gas productie bij de diverse clusters, en de aardbevingen in Groningen.

Uit de analyse blijkt dat er een duidelijke correlatie is in de zin dat voorafgaand aan aardbevingen er op de locatie van die aardbeving een signaal is te zien in de gasdruk in het reservoir. Dit is een her-analyse uitgevoerd in verband met een datalevering met betere, dagelijkse, tijdsresolutie van de reservoir gasdruk. Ook is er gebruik gemaakt van een verbeterde localisatie na her-analyse van de seismische data van een aantal van de aardbevingen in de KNMI catalogus.

English

This report is a continuation of research, commenced in 2014, which is part of a research project being carried out by Statistics Netherlands and commissioned by State Supervision of Mines (SodM). This research is part of the underpinning of the statistical methods employed to support the protocol for measurement and control of the production of natural gas in the province of Groningen. In this research the particular focus is on the relationship between reservoir gas pressure variations and the earth quakes in Groningen.

From the analysis it is clear that there is a correlation, in the sense that prior to earthquakes there is an enhanced signal in the reservoir gas pressure at the location of the earthquake. This is a re-analysis which is carried out because of the availability of improved, daily cadence, time series for the reservoir gas pressure. Also, use is made of improved localisation of a subset of earthquakes in the KNMI catalogue after re-analysis of the relevant seismometer traces.

1 Introduction

For some decades earthquakes of modest magnitudes have occurred in and around the Groningen gas field. It is recognized that quakes can be induced by the production of gas from a field eg. (Wetmiller, 1986); (Grasso and Wittlinger, 1990); (Bourne et al., 2014). An extensive study program is in place to improve the understanding of the risk and hazard due to gas production-induced earthquakes in the Groningen field (Nederlandse Aardolie Maatschappij BV, 2013).

The causality relationship between gas production and eartquakes is difficult to establish unequivocally, purely on the basis of time series analyses. For instance, a constant rate of gas extraction might lead to a likelihood of quakes that increases with time through the compaction of the reservoir layer, cf. (Bourne et al., 2014), but a correlation analysis would not necessarily provide any evidence of this. However, because in practice the rate of production does vary periodically throughout the year, as well as incidentally for operational reasons, it becomes

Figure 1.1 The locations of all quakes within the zone in Groningen relevant to this analysis, recorded after 1 January 1995. The red squares are locations of the production clusters, some of which are identified by name. The production field is also shown in dark gray, overplotted on a map of the region.

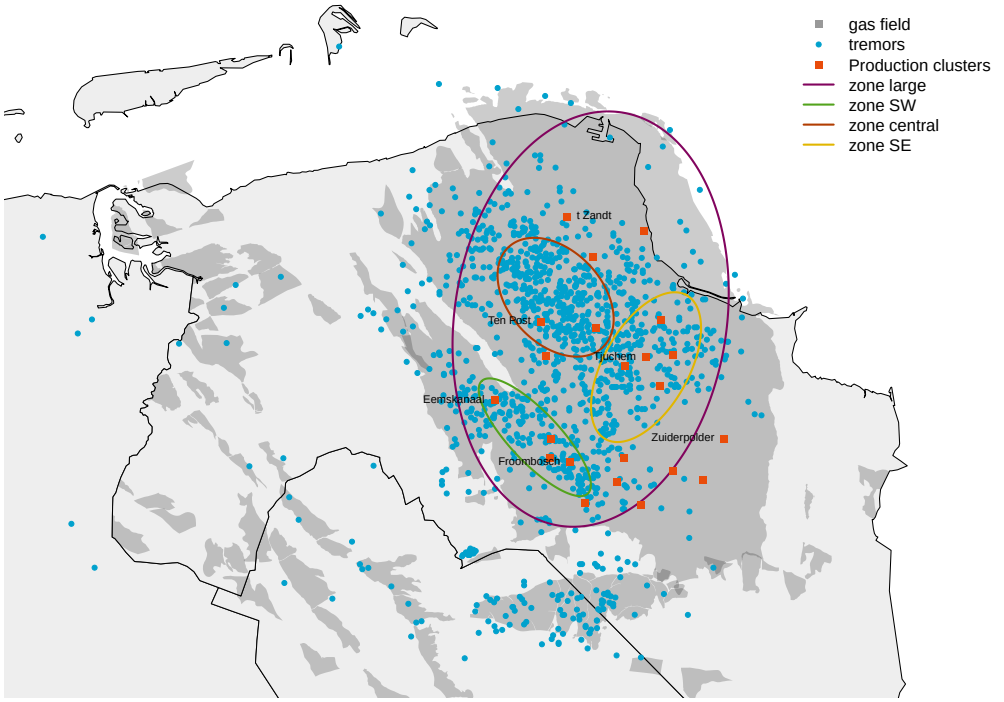

possible to pursue a correlation analysis between variations in quake incidence and production variations. Preliminary results on a correlation analysis between ground subsidence and production variations (Pijpers and van der Laan, 2015b) provide some support for the feasibility of this approach. There is no doubt that the extraction of natural gas strongly influences the balance of forces in the reservoir layers, eg. (Mulders, 2003). However, every quake is the realisation of a stochastic process, for which the balance of forces in part determines the probability distribution function of that process. Because of this stochasticity there is an intrinsic decorrelation between variations in gas production and variations in quake incidence frequency. Conversely, even if a correlation can be established between gas production and quake incidence, it will depend on the exact nature of that correlation whether causality can be considered proven or likely.

As with the CBS reports from the previous phases of this project, starting point for the analysis of the statistics of quakes is the catalogue of quakes as reported by the Royal Netherlands Meteorological Institute (KNMI) based on their processing of the network of seismometers that they manage. Further selections from that catalogue are made as necessary, for instance in order to filter out quakes that have occurred outside of the zone of interest, or quakes from an epoch when the seismometer network was less sensitive and may suffer from more serious completeness issues. The selection/filtering criteria are chosen to be consistent with those of the previous Statistics Netherlands reports, (Pijpers, 2014b), (Pijpers, 2015a), (Pijpers, 2015b): the spatial region of interest is the same as in those reports (see fig. 1.1). For a subset of 100 earthquakes that occurred after Jan. 1 2015, the original seismic data has been re-analysed, in order to improve the localisation. For the analyses in this report a set of 342 earthquakes, having occurred between Jan. 1 2014 up to the end of August 2017 is used. If an improved localisation is available from the re-analysis, this is used as data, if not then the original KNMI location is used.

The gas pressure inside the reservoir can be modelled, by making use of detailed geophysical mapping of the reservoir and its material properties, that together determine the diffusive flow of gas through the reservoir, induced by the gas production at the various clusters. In a previous report (Pijpers, 2015c), the gas flow induced by the gas production was modelled using a very simplified model of the flow, which did not take any variation of these material properties into account. Much better models are available however, in the form of the reservoir modelling tool MoReS (Por et al., 1989). In collaboration with TNO the MoReS code has been used to provide the starting point for an improved analysis. The reservoir gas pressure as a function of time at the required locations, ie. the locations of quakes and of a reference set of points, has been determined. These time series data are then combined in a way very similar to what is described in (Pijpers, 2015c) but without having to take recourse to the very simplified flow model used in that report.

The time resolution that MoReS can provide is very high. In a previous analysis (Pijpers, 2016) a relatively low time resolution of one week was used, to match the previous analysis of (Pijpers, 2015c). In the present paper the time resolution is daily. The pressure data used are weighted vertical averages inside the reservoir. The horizontal resolution of the numerical grid of MoReS varies, but is everywhere sufficient for the present analysis, since spatial uncertainties of less than about $500\ m$ are irrelevant given the uncertainty in localisation of quakes. The pressure data is therefore improved in accuracy. The localisation of the quakes has also been improved for a subset of earthquakes for which the original seismic data has been re-analysed. There will nevertheless still be a contribution to noise due to the uncertainty of localisation of quakes. Another source of uncertainty are the limitations of the modelling tool MoReS. While the model is calibrated with high frequency using borehole pressure data there are limitations in e.g. the resolution of the mapping of material properties of the reservoir.

2 Background

2.1 Propagation of the signal of gas extraction

In this view of the mechanism of induced earthquakes, it is not the case that the the variation in the rate of gas extraction, injects large amounts of potential energy into the reservoir which is accumulated and slightly later released suddenly as mechanical energy in the form of an earthquake. If that were the case a correlation analysis between variations in the production rate and the rate of energy release through earthquakes ought to be pursued. Rather, the view is that the potential energy is already present in the system, localised in particular at critically stressed fractures, built up over decades as the gas was removed from the reservoir. The history of gas extraction and the associated (differentiated) compaction of the fractured reservoir is responsible for the accumulation of this potential energy. As when tapping the first domino stone in a display of ever increasing numbers of falling dominoes, in this situation even a minor variation in gas pressure, or a spatial gradient of gas pressure (ie. a local forcing), might then cause a cascading energy release: an earthquake. The distribution function of the energy released in any given earthquake (ie. the slope in the Gutenberg-Richter plot) is likely to be influenced more by the (fractal) distribution of fracture sizes. In this scenario there is no reason to expect a clear correlation between gas pressure variations and the amount of energy released in any given quake. Instead the scenario should produce a correlation between gas pressure

variations and the rate of incidence of earthquakes (of any magnitude). For this reason the earthquake magnitude is only used as a data quality selection criterion to decide which earthquakes to include in the analysis.

It is clear that the locations of quakes do not coincide exclusively with the locations of the extraction clusters. If the gas extraction at the clusters is to have an influence at other locations, a signal has to pass from the well to those other locations. A signal occurs as gas diffuses through the reservoir layer, to replace the gas extracted at the well, or cluster of wells. A diffusive model for the signal of gas extraction has been used for instance by (Baranova et al., 1999) (their eq. 5) to model induced seismicity by hydrocarbon production in western Canada. A more general description can be found in (Russell and Wheeler, 1983). A controlling parameter for such diffusion is the diffusivity in the medium which is determined by material properties of both the medium and the material diffusing through it: the permeability of the medium and its porosity, the viscosity of the diffusing gas and its compressibility. None of these properties are constant throughout the region, and the system of larger and smaller faults also play an important role in channelling or obstructing flow. All of these factors are incorporated in a detailed finite-element model that is also calibrated on a regular basis by using a number of pressure measurement wells. For a description of the detailed modelling of the flow and pressure in the reservoir layers using MoReS the reader is referred to (Por et al., 1989) .

2.2 The local gas pressure history for quakes

In order to assess whether there is any kind of statistical correlation between the gas pressure throughout the Groningen field and the generation of quakes it is of interest to reconstruct the history of the gas pressure at the location of quakes in the period leading up to the time of the quake. It is assumed that the occurrence of quakes is not a fully deterministic process, but rather that an identical set of circumstances gives an identical finite likelihood for a quake to occur. A single event is then of limited value in terms of the information that it carries. Therefore one would wish to combine the history of every relevant quake to find the typical local gas pressure history for quake events. The dataset provided for the reservoir gas pressure has been generated using the MoReS code, with daily resolution starting on 1 January 2013. The time $T_{quake\ i}$ at which each quake occurs (identified with index i) is the reference value which is the 0-point for the shifting in time, and the reservoir pressure P as a function of time t is retrieved from the dataset for all selected quakes, with locations $(x_{quake\ i}, y_{quake\ i})$. This is done for all selected quakes after which straightforward averaging of the N time histories for every (selected) quake achieves the goal of obtaining the typical history of local gas pressure, and relative pressure variation before quakes as a function of 'look-back' time. This shifting and adding procedure is sometimes referred to as co-adding, i.e.:

$$P_{co-add\ real}(t) \quad = \frac{1}{N}\sum_{i=1}^{N} P_{reservoir}\left(x_{quake\ i}, y_{quake\ i}, (t - T_{quake\ i})\right) \tag{1}$$

Obtaining this averaged local pressure history for quakes is not yet sufficient for the purposes of the analysis. If instead of using locations and times of the selected quakes, one would pick an equal number of randomly chosen locations and times, a local pressure history could be obtained by applying the same technique of co-adding (i.e. shifting in time and averaging) of gas pressure histories.

$$P_{co-add\ synth}(t) \quad = \frac{1}{N}\sum_{i=1}^{N} P_{reservoir}\left(x_{synth\ i}, y_{synth\ i}, (t - T_{synth\ i})\right) \tag{2}$$

Since by definition such a randomly chosen set of locations and times is not special, it is only the differences between the histories of true quakes and artificial 'events' that is of interest. If the

co-added pressure history of true quakes turns out to be statistically indistinguishable from the co-added pressure history of random locations and times, no causality between gas pressure and quakes can be demonstrated by this route. To show the differences the ratio R is used, or the relative difference D:

$$R(t) \equiv \frac{P_{co-add\ quake}(t)}{P_{co-add\ synth}(t)}$$
$$D(t) \equiv 2\frac{P_{co-add\ quake}(t)-P_{co-add\ synth}(t)}{P_{co-add\ quake}(t)+P_{co-add\ synth}(t)} = 2\frac{R(t)-1}{R(t)+1} \quad (3)$$

In terms of methodology this approach of comparing a 'treatment' population (true earthquakes) with a non-treatment control population (random locations and times) is of course common in medical research whenever the effectiveness of new treaments or medication needs to be assessed. There in addition it is necessary to perform double blind testing in order to account for placebo effects which fortunately is not necessary here. The shift-and-add / 'co-adding' technique to extract a common behaviour or property, at as high as feasible signal-to-noise ratio, is borrowed from well-established astronomical imaging techniques (cf. Lynds et al. (1976); Christou et al. (1986)) which are still being used and developed further (e.g. Harpsøe et al. (2012)).

Figure 2.1 The rate of earthquakes calculated as a moving average with a window width of 270 days. This large width is to ensure sufficient statistics in the counts also for cutoff lower limits for the magnitude of $M = 1$ on the Richter scale. The dashes indicate the confidence limits on the rates, assuming Poisson statistics.

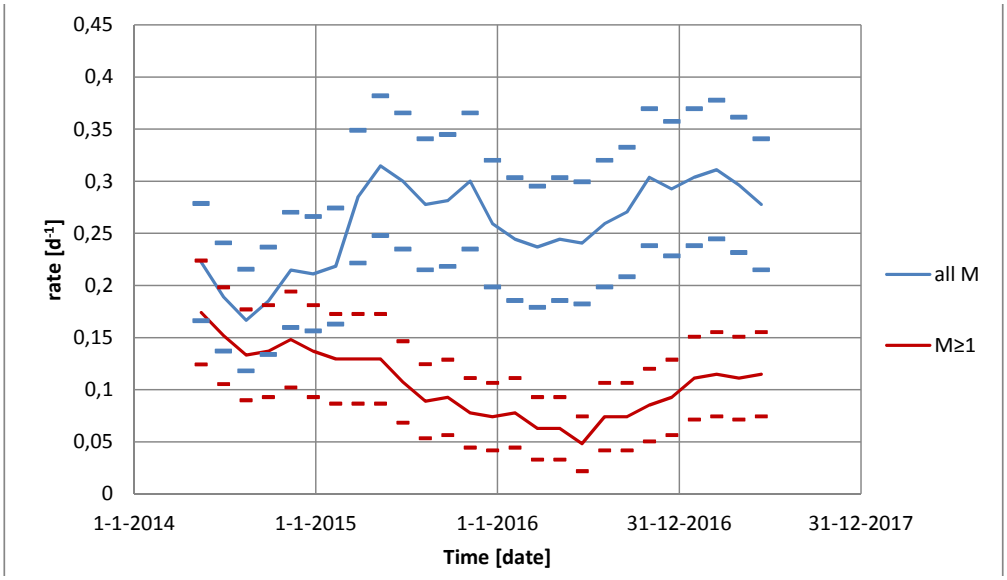

The analysis thus requires that a set of locations and times be set up, which can be used to build a local history of gas pressure in the same way that it is done for the true set of selected quakes. It might not be appropriate however to generate such a set using a completely uniform distribution over space or time. It is clear from fig. 1.1 that the spatial distribution of quakes is not uniform, and it is known that the distribution over time also is not completely uniform: see Fig. 2.1. It is desirable to mimic at least some aspects of the real distribution over space and time in the distribution for the set of artificial events. To this end the number of quakes in $2\ km \times 2\ km$ grid squares is counted. For the artificial events the number of events in each of these squares is reproduced, but random (x, y)—coordinates uniformly distributed within each grid square are generated. Similarly, for the timing of these artifical events, the full time range since Jan. 1 2014 is sectioned into intervals of length $50\ d$ and the number of true events in each

of these sections counted. The number of artificial events must match this true number but the actual timing within each subinterval is generated from a uniform distribution. In the following sections the plots are shown for a single realisation of random events.

Fig. 2.1 shows that the rate at which earthquakes are detected appears to vary with time. This rate is calculated as a moving average, counting earthquakes within a rather large window width of 270 days to ensure that there are a sufficient number of earthquakes to build up statistics, even with higher values for the cutoff limit for the earthquake magnitude. The particular choice of 270 days is a compromise between this requirement and the desire to retain some sensitivity to any seasonal component in the variations in earthquake rates (see also Pijpers (2017)). The uncertainties indicated by the dashes in Fig. 2.1 are calculated assuming that the statistics obey a Poisson distribution. While the stochastic process generating earthquakes probably does not satisfy the constraints of constant rate Poisson process, the margins do provide a reasonable guidance. Part of the full variation of rates is simply due to the stochastic nature of the process generating earthquakes. There is a downward trend of the rates for earthquakes with magnitudes above $M \geq 1$ on the Richter scale, at least up to late 2016, which is investigated recently in more detail and tested for statistical significance in eg. Pijpers and van Straalen (2017a) and Pijpers and van Straalen (2017b), which are the most recent updates of analyses that have been updated semiannually since late 2014. In particular when counting earthquakes with magnitudes above $M = 1$, the detection and localisation of earthquakes has been reliable for this entire period. If earthquakes with lower magnitudes are also included any downward trend is much less obvious: this is largely due to the much improved sensitivity over of the seismic detector network that KNMI has at its disposal since upgrades implemented over the course of 2015. Prior to that year, it is likely that the seismic network was insufficiently sensitive to have detected all earthquakes in the region with magnitudes below $M = 1$ or even $M = 1.2$. The detection completeness limit is now estimated to be nearer $M = 0.8$.

In the following section, the analysis is applied to 5 different selections from the earthquake catalogue:

1. All earthquakes in the catalogue in the period 1/1/2014 – 31/8/2017 : 342 earthquakes. This range is chosen because for each earthquake location and time there is at least 1 year of history of gas reservoir pressure available for the analysis.
2. All earthquakes in the catalogue in the period 1/9/2014 – 31/8/2017 : 291 earthquakes. The full range is shortened by 9 months, in line with the strategy of previous reporting where sections of 9 months are chosen as a compromise between sensitivity to seasonal effects and retaining sufficient data.
3. All earthquakes in the catalogue in the period 1/6/2015 – 31/8/2017 : 234 earthquakes. The range is shortened by another 9 months.
4. All earthquakes with M≥1 in the catalogue in the period 1/9/2014 – 31/8/2017 : 108 earthquakes. The period covered is the same as for set 2. above. The selection for magnitude should exclude earthquakes for which the localisation accuracy is sub-optimal.
5. All earthquakes with M≥1 in the catalogue in the period 1/6/2015 – 31/8/2017 : 70 earthquakes.

For each selection set of real data, a separate synthetic set is constructed.

3 Comparison of histories

3.1 All quakes after 1 January 2014

Figure 3.1 Left: a map of all selected earthquakes in set 1. On the right: the locations of artificial events set up as described in section 2.2 The indicated scales are in km. On the left are the true events in the same coordinate system

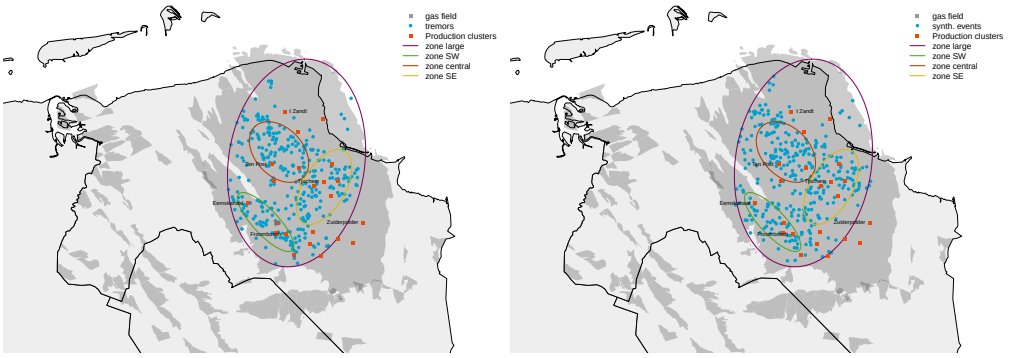

In the manner as described in section 2 in the first instance all quakes are selected having occurred within the relevant region andafter Jan. 1 2014, as indicated in fig. 1.1. For comparison the set of random synthetic events is shown in fig. 3.1. A total of 342 quakes (cq. events) is involved. The reservoir gas pressure at all locations in the reservoir decreases as a consequence of the gas extraction. At different locations in the reservoir the value of the gas pressure differs for any given calendar date. In the MoReS dataset used, the gas pressure is provided as a vertical volume average over the height within the reservoir, for all (X, Y) locations of the grid cells used in the code. For each real or synthetic quake location the nearest (X, Y) MoReS grid cell is selected.

Figure 3.2 The pressure as a function of calendar date, averaged for the locations of all 342 true quakes (blue line) and for the locations of all 342 synthetic events (red line).

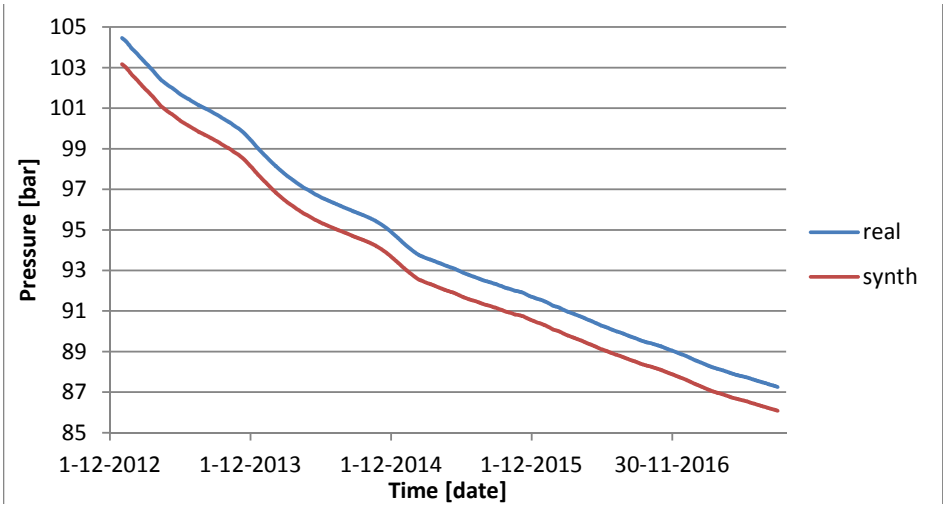

A straightforward average over all real quake locations, of the pressure on each calendar date from Jan. 2013 to Aug. 2017 is shown in Fig. 3.2. The same average pressure as a function of time for all synthetic locations is also shown. Clearly the pressure decrease, averaged over the 342 selected grid cells, is very similar as a function of time between the 342 locations of true

quakes, and the 342 locations of synthetic events, apart from an offset in pressure. The ratio of these two pressures, calculated for each day, is shown in the bottom panel of Fig. 3.2. This ratio varies irregularly with a full amplitude of about 0, 1% over the nearly 5 years covered.

Figure 3.3 The ratio of the averaged pressures as a function of calendar date. No shifting in time of the time series is applied here.

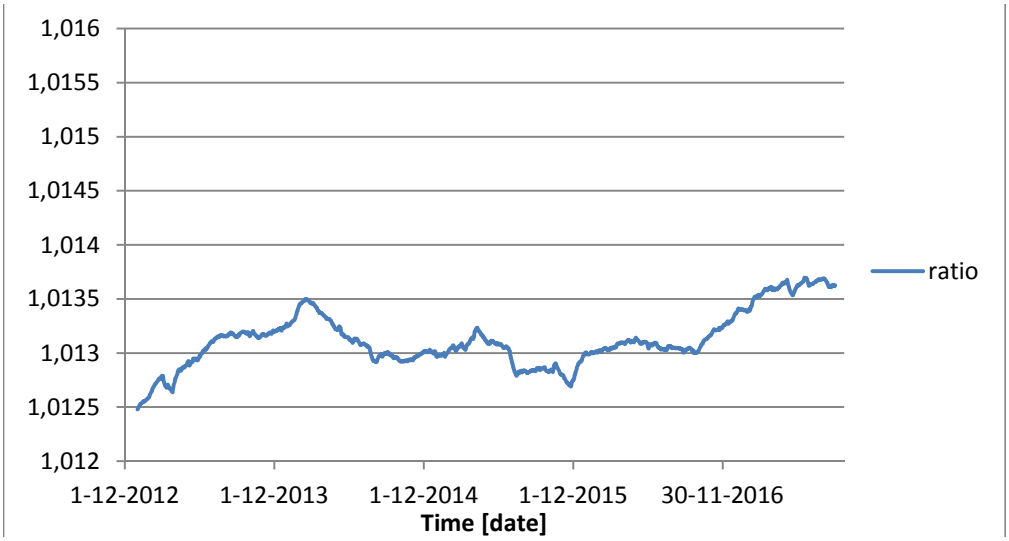

The next step is to repeat the procedure described in Pijpers (2016), which is to shift in time the pressure for each location (real or synthetic), so that the time of the events all coincide. Averaging the pressures after applying these shifts (see Eq. (1)) means that the average behaviour of the reservoir gas pressure in the time leading up to the event is obtained. By using pressure data from Jan. 2013 onwards, it is possible to determine for all quakes the reservoir gas pressure behaviour from at least 1 year before any of the events took place. This shift-and-averaging or co-adding is done for the 342 real earthquake events and for the 342 synthetic events, and shown in Fig. 3.4. Evidently the precursor pressure for real events (blue) and for synthetic events (red) decreases over the period of a year since the pressure trend is always downward throughout the reservoir. As with the usual average pressure shown before (Fig. 3.2) there is an overall offset in pressure. This offset is not of interest here because it is a consequence of using a single realisation of the synthetic events. It can be removed by dividing by the average pressure for the entire time period shown for each precursor pressure (real and synthetic).

Figure 3.4 Left panel: The co-added histories of gas pressure at locations of quakes (blue line) and at the set of synthetic events (red line), as a function of time leading up to the event (in days). Right panel: the ratio of the co-added histories of gas pressure variation prior to and at locations of real quakes and of synthetic events as a function of time (in days).

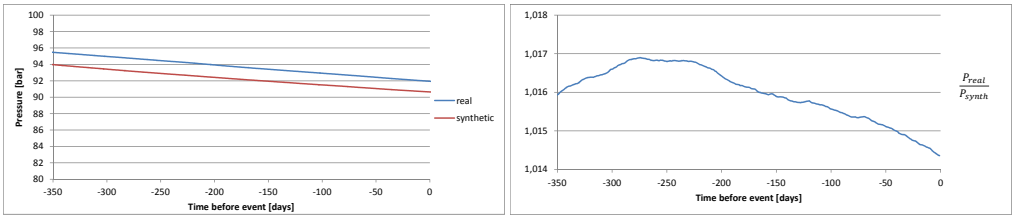

Fig. (3.5) shows the same precursor pressure with time, after normalization by the average for

Figure 3.5 Left panel: Each curve of the left panel of Fig. 3.4, normalized by its average value over the 350 day frame. Right panel: the ratio of these co-added histories of gas pressure variation prior to and at locations of real quakes and of synthetic events as a function of time (in days).

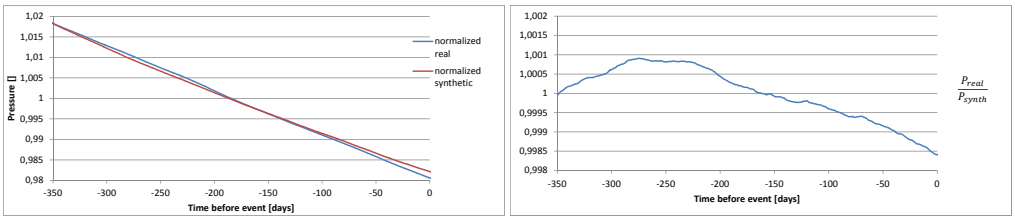

each curve. As is also pointed out in the previous report (Pijpers, 2016), it is the *difference* in behaviour with time between these two sets of events (real and synthetic) that is of interest here. The right hand panels in Fig. 3.4 and Fig. 3.5 show the ratio of the two curvesThe ratio of the (co-added) precursor pressures clearly shows a distinct systematic behaviour very different from the irregular behaviour of the bottom panel of Fig. 3.2. It is clear that at the locations of true events, the precursor pressure dips down more steeply than at random locations in the reservoir, with a full amplitude of some $0,25\%$ over roughly 220 days.

While not absolute proof, this gives a strong indication that the likelihood for a quake to occur reacts causally to gas production in the sense that locations of true quakes have a local pressure that decrease distinctly faster than the pressure for random locations. Fig. 3.3 shows that this is not due simply to the annual periodicity in production rates. While the local cluster production rates and therefore the gas reservoir pressure at any given location do have a seasonal component, the daily ratio after averaging over many locations (without time shifting) has no clear seasonal pattern, and the variations in this ratio within a year are considerably smaller as well as being much more irregular than what is seen in Fig. 3.5. Fig. 3.6 visualises these ratios in such a way that they can be shown on the same scale, from which the difference in behaviour is clear.

Figure 3.6 The difference between pressure history for true and synthetic events, divided by the average of the two. This is shown for the time-shifted 'co-added' time series, and also on the same scale for the average per calendar date without shifting. The latter is the same data as is shown in Fig. 3.3 but separately for every calendar year where $t = 0$ corresponds to Dec. 31 of that year.

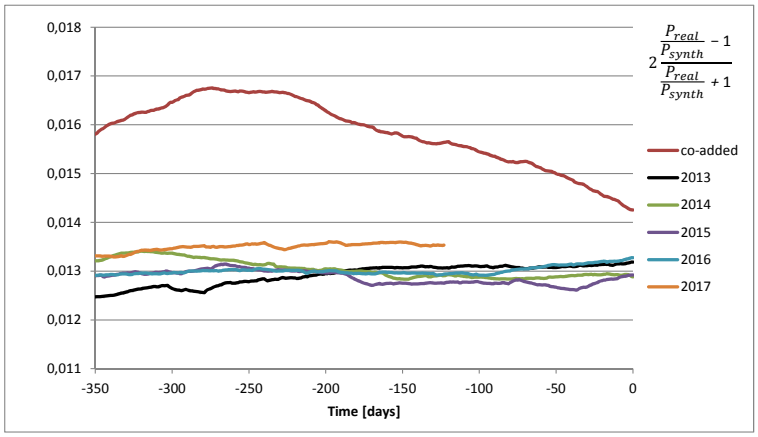

3.2 The epoch after 1 September 2014

In order to asses the influence of the period before 2015, when annual swings in production rate over the entire field were present, the data selection is adjusted. In this set, set 2, only earthquakes are selected which occurred after Sep. 1 2014, i.e. 9 months shorter than in section 3.1. In this set 2 a number of the earthquakes are less accurately localised earthquakes, in particular over the period of late 2014 and early 2015. Over the course of 2015 improvements were implemented by KNMI to the seismic detector network, installing many more detectors, spread out more evenly over the region. Until autumn of 2015, these were not yet fully operational. Since this poorer quality localisation might adversely affect the signal, a set with an additional selection criterion is analysed. For set 4 the same epoch is used as for set 2, but only earthquakes with magnitudes $M \geq 1$ are included, to reduce the influence of less accurately localised earthquakes.

Figure 3.7 Left panel: the ratio $R(t)$ for set 2. Right panel: the relative difference $D(t)$ for set 2, as well as this quantity for the averaging for each calendar date without shifting the pressure time series in time.

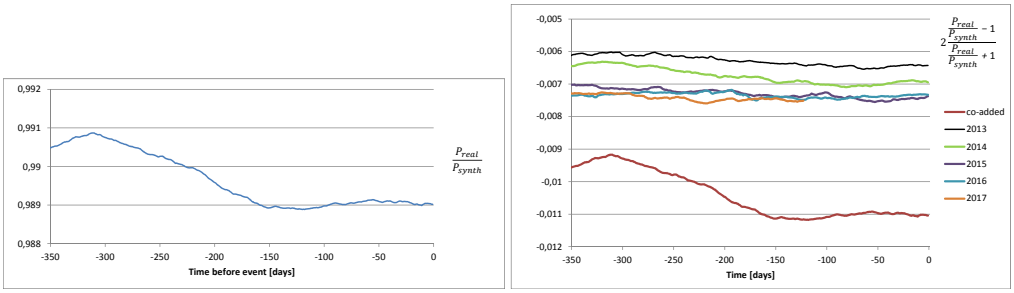

The right hand panels of Figs. 3.7 and 3.8 demonstrate that the behaviour with time of $D(t)$ is distinctly different from the averages without shifting to line up the earthquake timings. The behaviour of the reservoir gas pressure with time, leading up to earthquakes, is clearly different from that behaviour with time at random locations, since R is not constant for the co-added series. This is not due to foruitous selection of the synthetic set or a trivial propagation of seasonal production swings into the data, since the $D(t)$ calculated from the normal (unshifted) averages show no such behaviour. Comparing the left hand panels of Figs. 3.7 and 3.8 demonstrates that restricting the analysis to only the best localised earthquakes reveals a 'double hump' structure in $R(t)$. There was no evidence of this in previous analyses, going further back in time. The change in production strategy starting 2015 does appear to have changed the behaviour of the precursor pressure in the reservoir, but there continues to be a variation with time.

Figure 3.8 Left panel: the ratio $R(t)$ for set 4. Right panel: the relative difference $D(t)$ for set 4, as well as this quantity for the averaging for each calendar date without shifting the pressure time series in time.

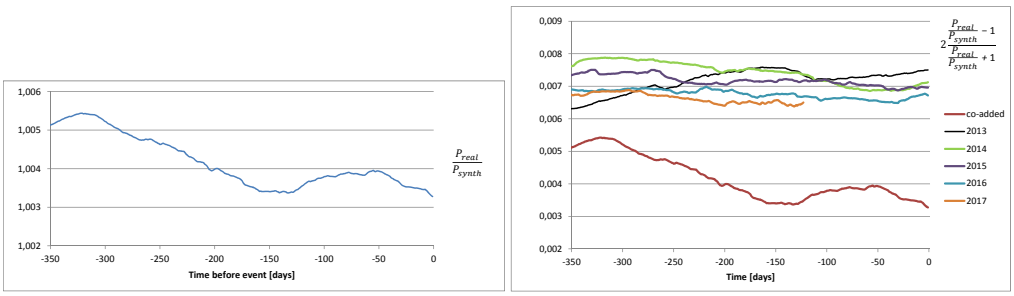

3.3 The epoch after 1 June 2015

The influence of the period before 2015 can be reduced even further by removing 9 more months at the beginning of the dataset. In this set 3, only earthquakes are selected which occurred after June 1 2015, i.e. a further 9 months shorter than discussed in section 3.2. For a separate set 5 the same additional selection criterion for earthquake magnitudes $M \geq 1$ is applied as is done in section 3.2, because even in this epoch the earthquakes with lower magnitudes are generally less accurately localised. Just as in the previous section the right hand panels of Figs. 3.7 and 3.8 demonstrate that the behaviour with time of $D(t)$ is distinctly different from the averages without shifting to line up the earthquake timings. The behaviour of the reservoir gas pressure with time, leading up to earthquakes, is clearly different from that behaviour with time at random locations, since R is not constant for the co-added series. Also, comparing the left hand panels of Figs. 3.9 and 3.10 demonstrates again that restricting the analysis to only the best localised earthquakes reveals a 'double hump' structure in $R(t)$.

Figure 3.9 Left panel: the ratio $R(t)$ for set 3. Right panel: the relative difference $D(t)$ for set 3, as well as this quantity for the averaging for each calendar date without shifting the pressure time series in time.

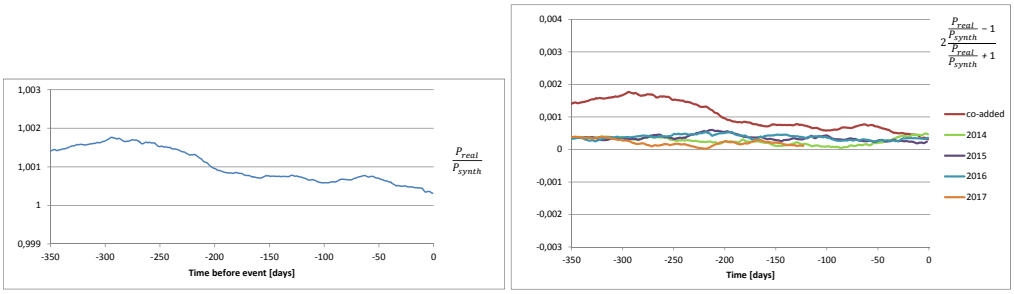

Figure 3.10 Left panel: the ratio $R(t)$ for set 5. Right panel: the relative difference $D(t)$ for set 5, as well as this quantity for the averaging for each calendar date without shifting the pressure time series in time.

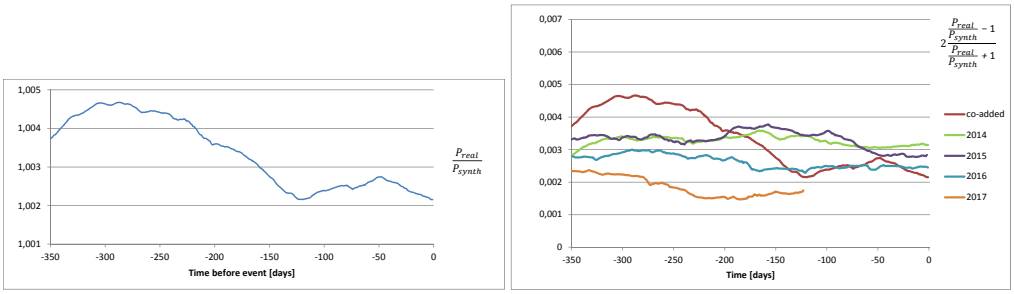

An analysis is still in progress to asses the statistical significance of these results. Such analyses were carried out for the previous datasets reported in (Pijpers, 2016) and showed a scaling of the signal-to-noise ratio roughly equal to the number of quakes used in the analysis. While that should in principle carry over, given that the methods are essentially the same, further checks are desirable.

4 Conclusions

There is a strong indication, already from (Pijpers, 2016), that the likelihood for earthquakes to occur reacts causally to gas production in the sense that variations in gas pressure in the reservoir, induced by variations in production rates, leads to an increased quake likelihood. Previous research (Pijpers, 2016) already indicated that pressure variations need to arrive at specific quake generating sites such as a faults or fractures. The improved time resolution of the reservoir gas pressure data available allows for an improved view of the precise behaviour of the reservoir gas pressure in the period leading up to a quake.

In the reports (Pijpers, 2014b), (Pijpers, 2015a), and (Pijpers, 2015b) it is demonstrated that a strong reduction in gas production at a number of clusters in the beginning of January 2014 was followed during that year by a reduction in frequency of quakes in the vicinity of those clusters, which is consistent with the time scale reported now. In work of (Pijpers, 2014a), (Pijpers and van der Laan, 2015a), (Pijpers and van der Laan, 2015b) a rapid response of the subsidence to production variations with a delay of about 9 weeks has been seen. Thus it would appear that production variations once propagated to the location of faults or fractures are followed by subsidence and the generation of quakes.

It is already pointed out in Pijpers (2016) that proof of causality requires the ability to exclude or identify the influence of all other possible factors that could affect the likelihood of quakes. In the case at hand an, as yet unidentified, external process that might explain the timing of quakes instead of the gas pressure would need to introduce an annual modulation. In addition this would have to be phased just right for the gas production variations propagated to quake sites to coincidentally line up in the period leading up to quakes, as well as phasing these to increase just before quakes. The present analysis does not give any reason to reject a hypothesis of (partial) causality through reservoir pressure variations induced by the gas production.

This behaviour is consistent with eg. the discussion in (Bourne et al., 2014), where it is the interaction of reservoir compaction, because of pressure depletion, with pre-existing faults and fractures that generates quakes. The locations of those pre-existing faults or fractures is then the relevant spatial characteristic of the quakes. The timing is important because it plays a role in 'lining up' in time gas pressure variations at the fracture locations. Within the context of critical systems, cf. (Main, 1995), one may hypothesize that the pressure depletion over long time scales has put the system of faults into a (nearly) critical state. The additional short term effect of production variations in this critical systems context might be that they act to push the system temporarily but repeatedly to a critical state and act as a trigger for quake avalanches.

It therefore appears that the current operationalisation of the gas production still produces substantial local variations in the reservoir gas pressure. The previous analyses (Pijpers, 2015b, 2016) suggested that pressure variations might act as a trigger on a critical system, so that sensitive locations (fractures) have an enhanced likelihood of producing an earthquake if they are subjected to such variations. Although the overall production rate has become more stable as a function of time, the reservoir gas pressure variations have not ceased. This is due to the variations in production rates at individual cluster locations. Such variations propagate into the reservoir and therefore there will continue to be variations in gas pressure throughout the reservoir which could act as earthquake triggers. Obtaining a more sustained further reduction in

quake incidence might require a combination of longer term reduction overall in production, as well as less variation in production rate at each individual cluster.

References

Baranova, V., A. Mustaqeem, and S. Bell (1999). A model for induced seismicity caused by hydrocarbon production in the western canada sedimentary basin. *Can. J. Earth Sci. 36*, 47--64.

Bourne, S., J. Oates, J. van Elk, and D. Doornhof (2014). A seismological model for earthquakes induced by fluid extraction from a subsurface reservoir. *J. Geophys. Res. 119*, 8991--9015.

Christou, J. C., E. K. Hege, J. D. Freeman, and E. Ribak (1986). Self-calibrating shift-and-add technique for speckle imaging. *Optical Society of America, Journal A 3*, 204--209.

Grasso, J. and G. Wittlinger (1990). 10 years of seismic monitoring over a gas field area. *Bull. Seismol. Soc. Am. 80*, 450--473.

Harpsøe, K., U. Jørgensen, M. Andersen, and F. Grundahl (2012). High frame rate imaging based photometry Photometric reduction of data from electron-multiplying charge coupled devices (EMCCDs). *Astronomy and Astrophysics 542*, A23 1--9.

Lynds, C., W. S.P., and H. J.W. (1976). Digital image reconstruction applied to alpha orionis. *Astrophysical Journal 207*, 174--180.

Main, I. (1995). Earthquakes as critical phenomena: Implications for probabilistic seismic hazard analysis. *Bull. Seismological Soc. Am. 85*, 1299--1308.

Mulders, F. (2003). Modelling of stress development and fault slip in and around a producing gas reservoir. Technical report, Delft University Press, Delft University, Netherlands.

Nederlandse Aardolie Maatschappij BV (2013). A technical addendum to the winningsplan Groningen 2013 subsidence, induced earthquakes and seismic hazard analysis in the Groningen field. Technical report.

Pijpers, F. (2014a). Phase 0 report 1 : significance of trend changes in ground subsidence in Groningen. Technical report, Statistics Netherlands.

Pijpers, F. (2014b). Phase 0 report 2 : significance of trend changes in tremor rates in Groningen. Technical report, Statistics Netherlands.

Pijpers, F. (2015a). Phase 1 update may 2015 : significance of trend changes in tremor rates in Groningen. Technical report, Statistics Netherlands.

Pijpers, F. (2015b). A phenomenological relationship between gas production variations and tremor rates in Groningen. Technical report, Statistics Netherlands.

Pijpers, F. (2015c). Trend changes in tremor rates in Groningen : update november 2015. Technical report, Statistics Netherlands.

Pijpers, F. (2016). A phenomenological relationship between reservoir pressure and tremor rates in Groningen. Technical report, Statistics Netherlands.

Pijpers, F. (2017). Supplementary material to cbs reports on earthquake frequencies. Technical report, Statistics Netherlands.

Pijpers, F. and D. van der Laan (2015a). Phase 1 update May 2015: trend changes in ground subsidence in Groningen. Technical report, Statistics Netherlands.

Pijpers, F. and D. van der Laan (2015b). Trend changes in ground subsidence in Groningen update November 2015. Technical report, Statistics Netherlands.

Pijpers, F. and V. van Straalen (2017a). Trend changes in tremor rates in Groningen : update june 2017. Technical report, Statistics Netherlands.

Pijpers, F. and V. van Straalen (2017b). Trend changes in tremor rates in Groningen : update october 2017. Technical report, Statistics Netherlands.

Por, G., P. Boerrigter, J. Maas, and A. de Vries (1989). A fractured reservoir simulator capable of modeling block-block interaction. Technical report, SPE Annual Technical Conference and Exhibition, 8-11 October, San Antonio, Texas.

Russell, T. and M. Wheeler (1983). *The Mathematics of Reservoir Simulation*. SIAM Frontiers in Applied Mathematics.

Wetmiller, R., . (1986). 'earthquakes near rocky mountain house, alberta, and their relationship to gas production. *Can. J. Earth Sci. 23*, 172--181.

Publisher
Statistics Netherlands
Henri Faasdreef 312, 2492 JP The Hague
www.cbs.nl

Prepress: Statistics Netherlands, Grafimedia
Design: Edenspiekermann

Information
Telephone +31 88 570 70 70, fax +31 70 337 59 94
Via contact form: www.cbs.nl/information

Where to order
verkoop@cbs.nl
Fax +31 45 570 62 68
ISSN 1572-0314